IOP Conf. Series: Journal of Physics: Conf. Series **853** (2017) 012002 doi:10.1088/1742-6596/853/1/012002

Dual frequency electrical impedance tomography to obtain functional image

Imam Sapuan*, Khusnul Ain, and Alif Suryanto

Department of Physics, Faculty of Sciences and Technology, Universitas Airlangga

*Corresponding email address: ispuan@yahoo.com

Abstract. Electric Impedance Tomography with two frequencies is a system to detect the anomalies. This system is expected to detect the presence of a cancer in the breast. In this study, the objects are modelled in a circle phantom within 13 cm diameter. Those objects are equipped with 16 electrodes of copperplate. The objects, carrots, are functioned as a cancer and water as a medium of the normal breast. This electrode works to inject the current and to measure the voltage at a certain point. The position of the electrode current injection is controlled by a de-multiplexer, whereas the measurement of voltage at the electrodes is controlled by a multiplexer. The electric current source utilized has two frequencies; 10 kHz and 100 kHz. This electric current is generated from a circuit of Voltage Controlled Current Source using an oscillator XR2206. The microcontroller is utilized to control the current injection through a de-multiplexer and the measurement of output voltage through a multiplexer.This research has produced three images. Two images are obtained from both frequencies of 10 kHz and 100 kHz. Those two images cannot be achieved in the reality. The object condition of normal breast cannot be measured, since the normal breast of a person is different from others. In this study, the two images can be obtained when the potential background of the phantom can be measured. The third image is obtained from the reconstruction of the electrical potential difference between the low and high frequencies. This image is called as a functional image. This functional image makes the EIT system can be implemented, since it can be obtained without measuring the potential background. This functional image reveals that the anomalies are more obvious than the single frequency image.

1. Introduction

Electrical impedance tomography (EIT) is a scanning technology using an electric current source to obtain an internal image of the object. The principle of tomography is to inject an AC current at the object through electrodes attached to the surface and to measure the electrical potential between the electrodes on the surface [1]. Electrical impedance tomography has the advantage to be safer for the body because it uses low electric current. The EIT system is also able to identify in the real time and is easy to be implemented because its creation is relatively simple [2].

The limitations of EIT system is firstly the low spatial resolution of the obtained image reconstruction. It is because of the limited number of electrodes that can be mounted on the surface of the object. The second drawback is that the injected current will be diffused into all directions, so the obtained potential data at the boundary is less sensitive or called as ill-pose conditions. The third drawback is the high noise of reached data measurement from the data signal cables, electrodes, and the movement of objects.

The third disadvantage can be overcome by making the scanning process at different frequencies. Data scanning at different frequencies can be reconstructed with a reconstruction method linearization. This reconstruction method produces significantly different conductivity other objects with other objects that are functional imagery.

One method of inverse problem can use linearization method. The linearization method assumes that the potential boundary alteration is a linear function of the conductivity alteration [3-4]. That linear function had been obtained by using Taylor series approach in $V(\gamma)$ around $V(\gamma_o)$ [5], namely:

$$V(\gamma) = V(\gamma_0) + V'(\gamma_0)(\gamma - \gamma_0) + O(\|\gamma - \gamma_0\|^2) \quad (1)$$

with $V'(\gamma_0)$ is Jacobion of $V(\gamma)$ on γ_0. By ignoring the last tribe, and then the equation (1) becomes

$$\delta V \approx J\delta\gamma \quad (2)$$

with $\delta V = V(\gamma) - V(\gamma_0)$, $J = V'(\gamma_0)$ and $\delta\gamma = \gamma - \gamma_0$.Jacobion is commonly referred as a matrix of sensitivity so that the equation (2) can be written in the form,

$$[\delta V]_{(q^2 x1)} = [S]_{(q^2 xp)}[\delta\sigma]_{(px1)} \quad (3)$$

with$[\delta V]$ is a potential alteration in the boundary, $[S]$ is the matrix sensitivity, and $[\delta\sigma]$ is the alteration of conductivity.

The relative imaging techniques require potential data comparator as a reference. References can be obtained from the data of potential object reference or the alteration of object conductivity since time t or object changes due to the frequency ω. The potential data of object reference is difficult to obtain, but the object of potential data during the conductivity changes related to the time or because the frequency is allowed to be enquiried. The potential data of object reference when the conductivity changes due to the time is called different time imaging, while the potential data of object reference when the conductivity changes because of the frequency is called imaging in the different frequency.

Different time imaging will produce functional image that can be used for physiological monitoring. The image is only relative image, not absolute image of $\sigma_{t,\omega}$ and $\omega\in_{t,\omega}$. This way is more real for applications compared to absolute imaging. In this different time imaging, the data obtained from two different time conditions is reduced to produce an image of admittance distribution alteration. By effectively reducing the data, it would effectively omit the error.

Different time imaging has shown the potential as a functional image in several areas of medical applications. If the potential data of different time imaging is not obtained, breast cancer imaging for instance [6-8], so the frequency of different imaging can be performed. The admittance spectrum of various biological tissues shows an alteration toward frequency [9-10]. Thus, that different frequency imaging is ascertained to generate an image of alteration of admittance distribution.

In the image of different frequency, image is built from the inverted projection algorithm of the ratio of two potential data in the different frequencies [11-13]. The sensitivity matrix method for algorithm reconstruction with the potential difference in the two frequencies can also be used [14-15]. Both of these methods in principally use the potential difference in the two frequencies and linear algorithm reconstruction.

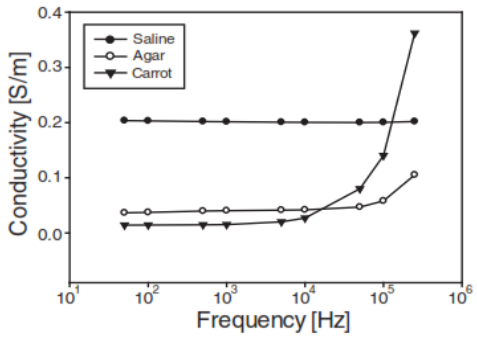

Figure 1.The conductivity of water (saline) with two objects, jelly and carrot [9]

Image with the different frequency using the potential difference weighted at two frequencies is easy to apply [17], for admittance spectrum of biological tissues alters toward frequency. It can be assumed that the image object with a frequency depends on the admittance of object reference. There are two different contrast mechanisms in the reconstructed image at different frequencies. First, there is a contrast in the admittance between the anomaly object and reference. The second, admittance distributions will alter toward frequency.

In this study, the carrot is used as the object of breast cancer, while the water represents the normal breast tissue. The carrot selection is based on the comparisons of different conductivity of carrot at frequency of 10 kHz and 100 kHz. According to research conducted by Zhao [16] at the frequency of 10 kHz and 100 kHz, the conductivity of carrots showed a very clear distinction.

Figure1. shows the different conductivity of carrot at 10 kHz and 100 kHz. Greater different conductivity between the carrots and water will produce higher contrast image. The frequencies used in this study are 10 kHz and 100 kHz. The source of electric currents is generated by current source circuit and the oscillator. The digital oscilloscope is used as an interface to display any potential difference of measurement results.

2. Research methods

In this research, the data collection process uses neighboring method. The phantom experiments use water and carrots as anomalies, elucidated in Figure 2. In this method, there are a pair of neighboring electrodes as flow injector and another pair of electrodes for measuring large voltages. Current injection is given by a pair of adjacent electrodes, while the potential difference is measured on all electrodes.

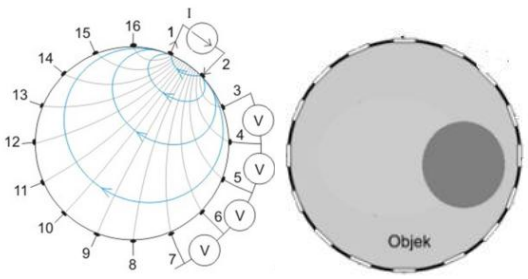

(a) (b)

Figure 2. (a) neighboring model (b) EIT Phantom model

The hardware of electrical impedance tomography system is composed of an oscillator circuit, a current source (VCCS), buffers, multiplexer, de-multiplexer and microcontroller. System hardware of electrical tomography system is revealed in Figure 3.

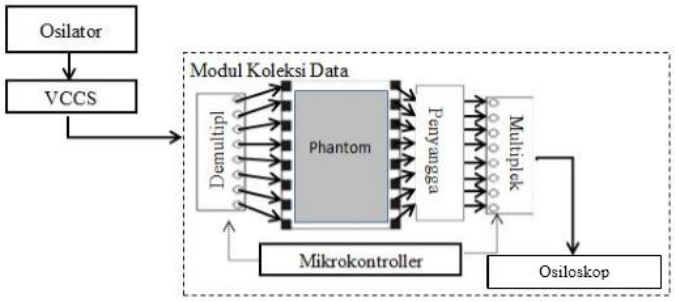

Figure 3. The electric impedance tomography system design

The oscillator is an electronic circuit that is able to generate an alternating current of electrical signal. IC oscillator circuit using XR-2206 can generate several types of waves, for instance, a square wave, triangular, and sinusoidal. XR-2206 circuit schematic is revealed in Figure 4.

By closing the switch of S_1, it will produce a sinusoidal signal on pin 2. The output frequency of this circuit can be determined by adjusting the value of the capacitor on pin 5 and resistor on pin 7. The frequency of the oscillator can be expressed by the following equation (4).

$$f = \frac{1}{RC}H \tag{4}$$

On pin 5 and 6, two capacitors are paralleled to adjust the frequency of the generated signal. Capacitor 470pF and 1nF is used for frequency 10 kHz or 100 kHz.

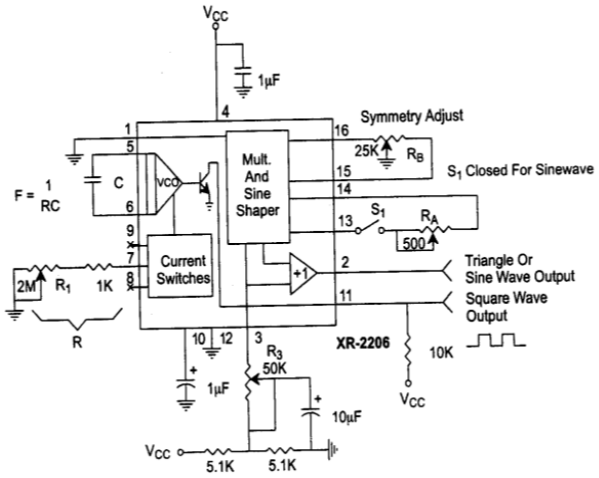

Figure 4. Schematic of IC XR-2206

Current source circuit or Voltage Controlled Current Source (VCCS) is a circuit that serves to maintain the stability of the current at a certain load range. This circuit serves to set the electrical current generated to be always constant when load is given. VCCS circuit schematic is shown in Figure 5.

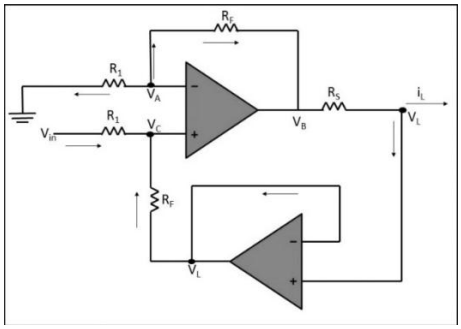

Figure 5. The circuit VCCS dual op-amp

VCCS circuit obtains the Vin input signal of the oscillator circuit and generates electric current Iout fixed I_{out}. This current will be injected into the object. The ideal I_{out} value is in accordance to the equation (5)

$$I_{out} = \frac{R_f}{R_s R_1} \times V_{in} \quad (5)$$

VCCS circuit uses the main component of op-amp of IC LM4562. This IC excellence compared to the op-amp IC LM741 or LM833 is more constant than current generated for greater load range. This is because the op-amp of IC LM4562 has very large output impedance. IC LM4562 has an impedance of 3000M Ohm while the LM741 has only 3M Ohm impedance.

The buffer circuit functions to maintain the measured voltage of the phantom, in order to avoid voltage drop when it is connected to the circuit in front of the circuit. Buffer circuit schematic is shown in Figure 6.

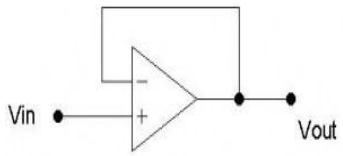

Figure 6. The simple buffer circuit

Due to the input voltage which is directly connected to the output, resulting output voltage will be equal to the input voltage (Vout = Vin).

Multiplexer can electronically be controlled to choose the activated path. One input of many inputs will be forwarded to the output. Selecting input is arranged by the control select. The multiplexer control the traffic signal of measurement result objects trough the electrode and the buffer to be forwarded to voltage measurement (digital oscilloscope) while the inversion of multiplexer is demultiplexer. Demultiplexer is used to regulate traffic flow injection to object through the connected electrodes.

Microcontroller is a device that is integrated into an IC to control electronic circuits. In this research, the type of microcontroller used is Atmega8535. This microcontroller controls in the current injection and voltage measurement via the multiplexer and demultiplexer. The minimum circuit system consists of four ports, namely ports A, B, C, and D. Table 1 shows the function of each - each port in this study.

PORT	Function	Interface
PA0 - PA7	Output	Demultiplexer
PB0 - PB7	Output	Multiplexer

Table 1. Pin Configuration Atmega8535 used

Image reconstruction is done by using Matlab software with the Filter Back Projection reconstruction methods. The algorithm method is based on the data collection through neighboring with circular geometry and based on equipotential. The algorithm of filtered Back Projection based on equipotential is initially proposed by Barber-Brown in matrix notation which can be expressed in the equation (6) [18].

$$[\delta\rho_n]_{(px1)} = [F]_{(pxp)}[B]_{(pxq^2)}[\delta V_n]_{(q^2x1)} \quad (6)$$

p is the number of elements and q is the number of electrodes, [B] is the weight matrix of Back Projection, [F] is the matrix representation of a filter, [δVn] are normalized limit of potential alteration, and [$\delta\rho n$] is normalized conductivity distribution alteration.

Linearization method assumes that the boundary of potential change is a linear function of the change in conductivity (Ain in 2014), so that equation (6) can be written in the form of a matrix that can be seen in equation (7).

$$[\delta V]_{(q^2x1)} = [S]_{(q^2xp)}[\delta\rho]_{(pxp)} \quad (7)$$

[δV] is a potential alteration of the boundary, [S] is the matrix sensitivities, and [$\delta\rho$] is the resistivity alteration. The step that could be done to acquire the matrix sensitivity [S] is by doing $\delta\rho$ variation on all elements in the equation (7).

Equation (7) may be completed after the matrix [S] is found by doing algebraic manipulations. However, since the matrix [S] is not square then [$\delta\rho$] cannot directly be obtained.

$$[S]^T{}_{(pxq^2)}[\delta V]_{(q^2x1)} = [S]^T{}_{(pxq^2)}[S]_{(q^2xp)}[\delta\rho]_{(pxp)} \quad (8)$$

$$[\delta V]_{(q^2x1)} = ([S]^T[S])^{-1}{}_{(pxp)}[S]^T{}_{(pxq^2)}[\delta\rho]_{(pxp)} \quad (9)$$

Generally [S] ^{T} [S] is a singular matrix so that the matrix has no inversion. To solve these problems, Tikonov regulation could be performed. Thus, the matrix will have the inversion.

$$[\delta V]_{(q^2x1)} = ([S]^T[S] + \alpha I)^{-1}{}_{(pxp)}[S]^T{}_{(pxq^2)}[\delta\rho]_{(pxp)} \quad (10)$$

α is a parameter of regulation and I is the identity matrix.

3. Results and discussion

The tomography hardware of electrical impedance with phantom experiments has been made as revealed in Figure 7

a

b

c

Figure 7. a. Electrical Impedance Tomography System
b. water reference c. phantom anomaly

3.1. Current injection module

Current injection module consists of an oscillator circuit and VCCS circuit. Based on the results having been obtained, an oscillator circuit is designed to fulfil the suitable frequency (10 kHz and 100 kHz) and required amplitude of 0.78 volts (2Vpp) with a sinusoidal output signal.

The constant current source (VCCS) that had been made is capable of producing a constant current 0.0057 A for the range of 155-560 ohm load and a frequency of 10 kHz. This testing was conducted on a VCCS input voltage of 0.7 volts (2Vpp). The data and graphics of current stability are elucidated in Table 2 and Figure 8.

This VCCS circuit is also capable of producing a constant current 0.0035 A for the range load of 300-621 ohm and a frequency of 100 kHz. The testing was conducted on a VCCS circuit with an input voltage of 0.35 volts (1Vpp). The data and graphics of current stability are elucidated in Table 3 and Figure 9.

The constant current source that had been made is suitable with the needs of current of the EIT system in milliamps. The resulted current is still safe when applied to the human body because it is below 10 mA.

Resistance (Ohm)	Voltage (Volt)	Current (mA)
101	0.7071	0.0070
155	1.0607	0.0058
243	1.4142	0.0058
303	1.7678	0.0058
364	2.1213	0.0058
436	2.4749	0.0057
498	2.8284	0.0057
562	3.1820	0.0057
687	3.5355	0.0051

Table 2. The data of circuit voltage test results with 10kHz frequency to the load

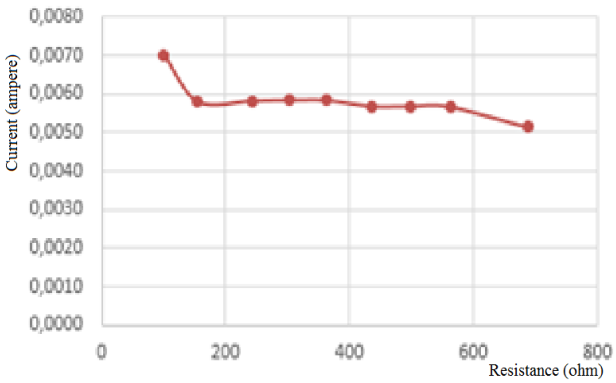

Figure 8. The graph of the relationship between output current to the load, at a frequency of 10kHz.

Resistance (Ohm)	Voltage (Volt)	Current (mA)
98	0.3536	0.0036
158	0.7071	0.0045
300	1.0607	0.0035
407	1.4142	0.0035
526	1.7678	0.0034
621	2.1213	0.0034
760	2.4749	0.0033

Table 3. The data from current source circuit testing at frequency of 100 kHz to the load

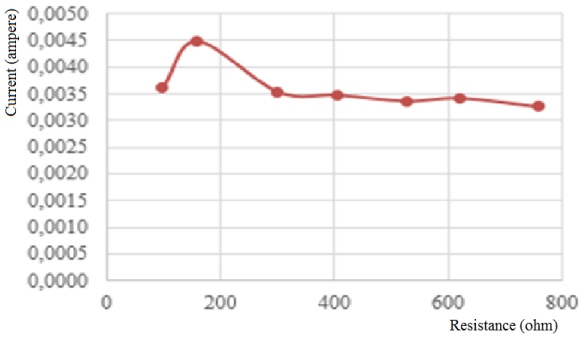

Figure 9.The graph of the relationship between the output current to the load at a frequency of 100 kHz

3.2. Voltage measurements

Hardware measuring the voltage that has been made is shown in Figure 7. This hardware consists of several components including a phantom, buffer circuit (buffer), multiplexer circuit, and microcontroller.

The process of voltage measurement in this research is controlled by a microcontroller circuit. This circuit serves to regulate the flow of the VCCS injection process via demultiplexer which is connected to the electrode. The microcontroller also regulates the voltage measurement process which is done through a multiplexer that is connected to the electrode.

3.3. Analysis of the collected data

In this research, the process of collecting data is done by using the electrode for 16 units. The first step starts from currents injected in the electrodes 1 and 2, where as a current injection electrode 1 and 2 as a ground electrode. Data retrieval is done on the potential difference electrode pairs 1 and 2, 2 and 3, 3 and 4, until the data to 16 is a pair of electrodes 16 and 1. This process is repeated until the current injection to 16 (the pair of electrodes 16 and 1), so that the amount of data obtained on measuring the potential difference of 256 data.

Potential measurements made on two State phantom, i.e. normal (water reference) and anomalies (water + carrots). Each measurement is performed in the same manner at a frequency of 10 KHz and 100 kHz. The graph of the results of the measurements of potential difference with 16 electrodes at water reference is shown in Figure 10. The graphs of measurement results of potential difference with 16 electrodes on the phantom breast cancer anomaly are as shown in Figure 11.

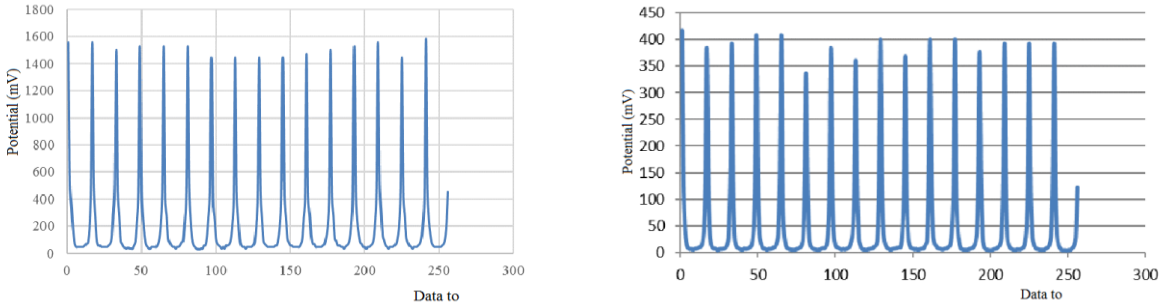

(a) (b)

Figure 10. The graph is results of the measurements of potential difference with 16 electrodes at water reference. (a) The frequency of the10kHz, (b)The frequency of the 100kHz

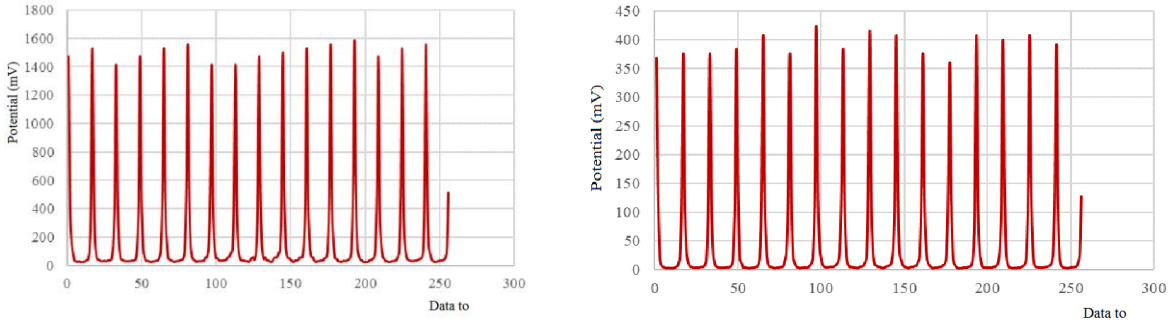

(a) (b)

Figure 11. The graph results on the measurements of potential difference with 16 electrodes at water reference. (a) The frequency of 10 kHz, (b) The frequency of 100 kHz.

Voltage measurements is performed on a phantom object made of water as a media and a normal object or as a background while the water as well as carrot acts as a representative of anomalous objects. Data collection was performed twice, for current injection frequency of 10 kHz and 100 kHz. These measurements performed at a frequency of 10 kHz produces a potential difference which is relatively higher compared with measurements made at a frequency of 100 kHz. This is because the magnitude of the potential difference measured is inversely proportional to the frequency used, as shown by the following equation.

$$V = I.Z = I\,.\sqrt{R^2 + \left(\frac{1}{2\pi f.C}\right)} \tag{11}$$

3.4. Image reconstruction results

There were three images obtained in the reconstruction process as shown in Figure 12. Image reconstruction method used equation (11). Two images were reconstructed from the data electric potential difference of the background and background + anomalies. Background electric potential is an electric potential measured in the water phantom object. Whereas, electric potential of background + anomaly is the electrical potential measured at the water + carrot phantom object.

Image (a) was obtained from the data reconstruction of electric potential difference between the background with background + carrot on the current frequency of 10 kHz. Whereas, Image (b) was obtained from the data reconstruction of electric potential difference between the background with background + carrot on the current frequency of 100 kHz

The both-images are relative images. Assuming that the change of potential boundary is a linear function of the change in conductivity, those two images cannot be achieved in the reality. The object condition of normal breast cannot be measured, since the normal breast of a person is different from others. In this study, the two images can be obtained if the potential background of the phantom can be measured.

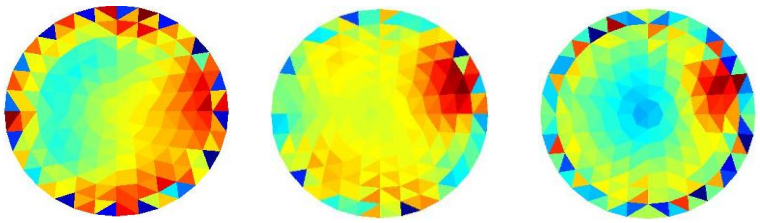

Figure 12.Image Reconstruction resulted on (a) reconstructed image at frequency of 10 kHz between phantom with the water reference, (b) reconstructed image at frequency of 100 kHz between phantom with the water reference, and (c) the results of image reconstruction of the electric potential difference of water + carrot on 10kHz and 100kHz.

The third image was obtained from the reconstruction of the electrical potential difference between the low and high frequencies. This image is called as a functional image. This functional image makes the EIT system can be implemented, since it can be obtained without measuring the potential background. This functional image reveals that the anomalies are more obvious than the anomalies in the single free frequency image.

4. Conclusion

Based on the results of the conducted research, it can be summarized as follows:

1. Electrical Impedance Tomography systems (EIT) Dual frequency with several constituent components, like the circuit: oscillator, Voltage Controlled Current Source (VCCS), buffer, current injection and voltage measurement, as well as neighboring method for current injection process and measurement potential difference has successfully created.
2. Electrical Impedance Tomography System (EIT) has been successfully tested in water as medium and carrots as the object of breast cancer. Functional image reconstruction is obtained from the difference of electrical potential for low and high frequencies. With functional system image, EIT can be applied in the reality, because without doing the measurement the image background can be obtained. This functional image shows the anomaly clearly more than anomaly on the image of a single frequency**.**

Reference

[1] Ain K, Sapuan I, Wibowo R A, Kurniadi D2012 Electric Impedance Tomography System for Nondestructive test of Simple, University of Airlangga
[2] Setiyanto D 2011 Design and Buildingof Prototype Elektrical Impedance Tomography(EIT) with Single Frequency, Faculty of Mathematic dan Natural sciences, University of Indonesia
[3] Borsic A 2002 Regularisation Methods for Imaging from Electrical Measurements, A thesis of Philosophy Doctor, Oxford Brookes University
[4] Chen X Y, Wang H X, Newell J C 2011 Lung Ventilation Reconstruction by Electrical Impedance Tomography Based on Physical Information *3rd International Conf. on Measuring Technology and Mechatronics Automation IEEE Computer Society*
[5] Noor A 2007 Electrical Impedance Tomography at Low Frequencies *Thesis of Doctor Phylosophy* University of New South Wales
[6] Kukarni R, Boverman G, Isaacson D, Saulnier G J, Kao T J, Newell J C 2008 An analytical layered forward model for breast in electrical impedance tomography *Physical Measurement* **29** S27-S40
[7] Soni N K, Hartov A, Kogel C, Poplack S P, Paulsen K D 2004 Multi-frequency electrical impedance tomography of the breast : new clinical results *Physical Measurement* **25** S301-

S314
[8] Trokhanova O V, Okhapkin M B, Korjenevsky A 2008 Dual-Frequency Electrical Impedance Mammography For The Diagnosis of Non Malignant Breast Desease *Physical Measurement* **29** S331-S334
[9] Gabriel C, Gabriel S, Carthout E, 1996 The dielectric properties of biological tissues : I : literature survey *Physical Medical Biology* **41** pp 2231-2249
[10] Oh T I, Koo W, Lee K H, Kim S M, Lee J, Kim S W, Seo J K, Woo E 2008 Validation of Multi-Frequency Electrical Impedance Tomography (Mfeit) System KHU Mark I *Impedance Spectroscopy And Time Difference Imaging, Physical Measurement* **29** S295-S307
[11] Griffith H 1987 The Importance Of Phase Measurements In Electrical Impedance Tomography *Physical Medical Biology* **32** pp 1435-1444
[12] Griffith H and Zhang Z 1989 A Dual-Frequency Electrical Impedance Tomography System *Physical Medical Biology* **34** pp 1465-1476
[13] Schlappa J, Anesse E, Griffiths H 2000 Systematic Error In Multi Frequency Electrical Impedance Tomography Of The Breast *New Clinical Results, Physical Measurement* **21** S111-S118.
[14] Romsauerova A, Mc Ewan A, Horesh L, Yerworth R, Boyford R H, Holder D 2006 Multi-Frequency Electrical Impedance Tomography (EIT) Of The Adult Human Head : Initial Finding In Brain Tumor, Arteriovenous Malformations And Chronic Stroke, Development of An Calibration *Physical Measurement* **27** S147-S161
[15] Yerworth R J, Bayford R H, Brown B, Milnes P, Conway M, Holder D 2003 Electrical Impedance Tomography Spectroscopy (EITS) for Human Head Imaging *Physical Measurement* **24** S477-S489
[16] Zhao *et al.* 2012 High Density Trans-admittance Mammography Development and Preliminary Phantom Tests, Kyung Hee University, Yongin-si, Gyeonggi-do, 446-701
[17] Seo J K, Lee J, Kim S W, Zribi H, Woo E J 2008 Frequency Difference Electrical Impedance Tomography (Fdeit) Algorithm Development And Feasibility Study *Physical Measurement* **29** S929-S944
[18] Ain K 2014 Tomografi of Dual modality Electrical And Acoustical Properties To Increase Image Quality *Dissertation Department Of Engineering Physics ITB Bandung*
[19] Bera T K, Nagaraju J, Lubineau G 2016 Electrical Impedance Spectroscopy (EIS)-Based Evaluation Of Biological Tissue Phantoms To Study Multifrequency Electrical Impedance Tomography (Mf-EIT) Systems *Breast Cancer,Facts & Figures*
[20] Zhang J, Patterson R P, Koqenevsky A 2002 Comparison and Analysis of Electrical Impedance Tomographic Images Reconstructed Using Two Algorithms *Proc. of the Second Joint EMBS/BMES Conference*